J Antimicrob Chemother 2016; **71**: 1933–1942
doi:10.1093/jac/dkw050 Advance Access publication 29 March 2016

Journal of Antimicrobial Chemotherapy

Population pharmacokinetic analysis of elvitegravir and cobicistat in HIV-1-infected individuals

Catalina Barceló[1], Frédéric Gaspar[2], Manel Aouri[1], Alice Panchaud[2], Margalida Rotger[1,3], Monia Guidi[1,2], Matthias Cavassini[4], Thierry Buclin[1], Laurent A. Decosterd[5] and Chantal Csajka[1,2]* on behalf of the Swiss HIV Cohort Study†

[1]Division of Clinical Pharmacology, University Hospital Centre and University of Lausanne, Lausanne, Switzerland; [2]School of Pharmaceutical Sciences, University of Geneva, University of Lausanne, Geneva, Switzerland; [3]Institute of Microbiology, University Hospital Centre and University of Lausanne, Lausanne, Switzerland; [4]Service of Infectious Diseases, University Hospital Centre and University of Lausanne, Lausanne, Switzerland; [5]Innovation & Development, Laboratory of Clinical Pharmacology, Service of Biomedicine, University Hospital Centre and University of Lausanne, Lausanne, Switzerland

*Corresponding author. Division of Clinical Pharmacology and Toxicology, University Hospital Centre (CHUV), Bugnon, 17 Lausanne 1011, Switzerland. Tel: +41-21-314-42-60; Fax: +41-21-314-42-66; E-mail: chantal.csajka@chuv.ch
†Members are listed in the Acknowledgements.

Received 13 October 2015; returned 16 November 2015; revised 15 January 2016; accepted 5 February 2016

Objectives: Co-formulated elvitegravir, cobicistat, tenofovir disoproxil fumarate and emtricitabine is among the preferred regimens for first-line ART. A population approach was used to characterize the pharmacokinetics of elvitegravir and cobicistat and identify individual factors and co-medications influencing their disposition, taking into consideration the interaction between the two compounds.

Methods: The study population included 144 HIV-infected individuals who provided 186 and 167 elvitegravir and cobicistat plasma concentrations, respectively. First, distinct NONMEM® analyses were conducted for elvitegravir and cobicistat, including individual demographic, clinical and genetic factors as potential covariates. Elvitegravir and cobicistat interaction was then assessed through different inhibitory models. Simulations based on the final model served to compare expected drug concentrations under standard and alternative dosage regimens.

Results: Clearance with between-subject variability was 7.6 L/h [coefficient of variation (CV) 16.6%] and volume of distribution 61 L for elvitegravir and 16.0 L/h (CV 41.9%) and 88.3 L, respectively, for cobicistat. Concomitant administration of non-ritonavir-boosted atazanavir decreased elvitegravir clearance by 35%, likely due to UDP-glucuronosyl transferase (UGT) 1A1 inhibition. Concomitant administration of non-ritonavir-boosted atazanavir and ritonavir-boosted darunavir decreased cobicistat clearance by 47% and 27%, respectively. The final interaction model included cobicistat exposure (AUC_{0-24}) on elvitegravir clearance. Simulations confirmed that a reduced elvitegravir dose of 85 mg co-administered with cobicistat and atazanavir produces a concentration–time course comparable to the standard regimen without atazanavir.

Conclusions: Elvitegravir and cobicistat pharmacokinetic variability appears to be mainly explained by drug–drug interactions that may be encountered in routine clinical practice. In these cases, therapeutic drug monitoring and surveillance for potential toxicities would be justified.

Introduction

The once-daily fixed-dose combination containing elvitegravir boosted with cobicistat, tenofovir disoproxil fumarate and emtricitabine is among the preferred regimens for first-line ART and a switch option for experienced individuals according to HIV guidelines.[1–8] The integrase strand transfer inhibitor elvitegravir is also available as a stand-alone agent to be co-administered with other antiretroviral agents, combined with ritonavir or cobicistat.[9]

Elvitegravir undergoes biotransformation via cytochrome P450 3A (CYP3A) and to a lesser extent via UDP-glucuronsyl transferase (UGT) 1A1 and 1A3.[10–12] Cobicistat is a novel pharmacokinetic boosting agent; it is a structural analogue of ritonavir without antiretroviral activity. It has higher specificity for inhibiting CYP3A4/3A5 and is also used to boost the PIs atazanavir and darunavir.[13,14] CYP3A4 and CYP2D6 are the enzymes involved in cobicistat metabolism. Cobicistat also inhibits, though weakly, CYP2D6 and efflux transporters such as P-glycoprotein, breast cancer

resistance protein (BCRP) and organic anion-transporting polypeptides (OATPs) 1B1 and 1B3.[15–17]

Population pharmacokinetic analyses conducted with pooled data from clinical studies in healthy and HIV-infected individuals reported moderate between-subject variability [coefficient of variation (CV)] in clearance, reaching 29%–32% for cobicistat- or ritonavir-boosted elvitegravir and 53% for cobicistat.[18,19]

Although combination of co-formulated elvitegravir and cobicistat with other antiretroviral agents, such as ritonavir-boosted or non-boosted PIs, is not recommended, they are sometimes used in routine clinical practice to treat complicated HIV infections. Their mutual influence on each other's concentrations is unknown and there are no dosing adjustment recommendations. Therefore, the characterization of their pharmacokinetic variability and assessment of potential drug–drug interactions outside a clinical trial setting is of relevance for clinical practice. The objective of this study was to develop a population pharmacokinetic model for elvitegravir and cobicistat in a cohort of HIV-1-infected individuals, to quantify the interaction between the two compounds and to identify potential factors influencing elvitegravir and cobicistat disposition.

Methods

Study population

Elvitegravir plasma concentrations were obtained from 144 HIV-infected individuals within the frame of therapeutic drug monitoring (TDM) performed at the University Hospital Centre of Lausanne between February 2011 and February 2015. Cobicistat plasma concentrations were measured in 133 of these individuals. A median of one sample per individual (range one to five) was collected between 0.5 and 27.75 h after the last dose intake under steady-state conditions. All participants received a fixed-dose combination containing 150 mg of elvitegravir, 150 mg of cobicistat, 300 mg of tenofovir disoproxil fumarate and 200 mg of emtricitabine in a single tablet, once daily. Exclusion criteria were undetectable elvitegravir and cobicistat plasma concentrations, suggestive of non-adherence to treatment, and non-reliable time information about blood sampling or last dose intake. This study was conducted within the frame of the Swiss HIV Cohort Study (SHCS) (http://www.shcs.ch).

Analytical method

Plasma level measurements were performed in the Laboratory of Clinical Pharmacology at the University Hospital Centre of Lausanne. Plasma samples obtained from HIV-infected individuals were isolated by centrifugation and stored at −20°C until batch analysis. On the day of the analysis, samples were inactivated for virus at 60°C for 60 min. Plasma elvitegravir and cobicistat levels were determined by LC–MS/MS after protein precipitation with acetonitrile according to our previously reported analytical method, which was adapted to include cobicistat.[20] The method showed acceptable precision (inter-day CV 3–6.3%) and accuracy (CV 3.8–7.2%). The calibration curves of elvitegravir and cobicistat are linear, with a lower limit of quantification (LLOQ) of 50 and 5 ng/mL, respectively. The laboratory participates in an international external quality assurance programme for antiretroviral drug analysis (KKGT, Stichting Kwaliteitsbewaking Klinische Geneesmiddelanalyse en Toxicologie, Association for Quality Assessment in TDM and Clinical Toxicology, The Hague, The Netherlands, http://www.kkgt.nl/).

Genotyping

We selected the genetic variant *UGT1A1*28* (rs8175347) with a proven loss-of-function effect and minor allelic frequency >0.05.[21–23] We successfully genotyped 56 of the 60 SHCS participants that gave genetic consent. Genotyping was performed by direct sequencing as previously described.[24] We verified that the variant studied was in Hardy–Weinberg equilibrium.

Population pharmacokinetic analysis

Non-linear mixed-effects modelling was performed with NONMEM® (version 7.1.0, ICON Development Solutions, Ellicott City, MD, USA). First, distinct pharmacokinetic models for elvitegravir and cobicistat were built based on natural log-transformed plasma concentrations. Then, a simultaneous model describing the influence of cobicistat on elvitegravir oral clearance was developed, while considering covariates potentially influencing the pharmacokinetics of each drug.

Structural models

A stepwise procedure was used to identify models that best fitted elvitegravir and cobicistat data, testing one- and two-compartment models with first and/or zero-order absorption with and without absorption lag time. Since elvitegravir and cobicistat are administered orally, apparent clearance (CL/*F*) and volume of distribution (*V*/*F*) were estimated (where *F* is the absolute oral bioavailability).

Statistical models

Exponential errors following a log-normal distribution were assumed for the description of between-subject variability of the pharmacokinetic parameters, described by the equation $\theta_j = \theta \times e^{\eta_j}$, where θ_j is the individual pharmacokinetic parameter of the *j*th individual, θ is the geometric average population value and η_j is a between-subject random effect, which follows an independent, normal distribution with mean zero and variance ω^2. A combined proportional and additive error model was used to depict residual variability.

In the cobicistat model, different approaches to the management of data below the limit of quantification (BLQ) were tested, but likelihood-based methods failed to achieve successful minimization.[25–28] We performed a sensitivity analysis between two standard methods corresponding to the exclusion of the BLQ measurements (M1) and imputation to half the LLOQ (M5).[25] We examined whether the BLQ data treatment affected the estimates. Finally, method M5 was used to treat BLQ data and a fixed additive variance component, corresponding to half the LLOQ, was incorporated into the error model.

Covariate models

The correlation between elvitegravir and cobicistat individual pharmacokinetic estimates and demographic, clinical and genetic covariates was first explored graphically to identify potential and physiologically plausible relationships. Then, covariate analysis was performed using a stepwise insertion/deletion approach testing linear or non-linear functions as appropriate (categorical covariates coded as 0 and 1, continuous covariates centred on their median value). Missing values were imputed to the population median value for continuous covariates. To avoid a possible bias in the covariate analysis due to missing covariates, subset analyses including only individuals with available data were performed and results were compared with the original dataset. Sex, body weight, height, body surface area, co-medications and *UGT1A1*28* (rs8175347) genotype were tested as covariates on elvitegravir pharmacokinetics. Genotyped individuals were classified into three groups: homozygous for the reference allele (*UGT1A1*1/*1*); heterozygous (*UGT1A1*1/*28*); and homozygous for the rare allele (*UGT1A1*28/*28*). Individuals with missing genotype results were treated as a fourth group. Rich and reduced models were tested to estimate the impact of the genetic variant on individual elvitegravir pharmacokinetic parameters. Rich models allowed *UGT1A1*1/*1*, *UGT1A1*1/*28*, *UGT1A1*28/*28* and the missing genotype group to have

different values of the parameter. In reduced models, genotypes with similar parameter estimates were grouped in a unique variable. Sex, body weight, height, body surface area and co-medications were tested as covariates on cobicistat pharmacokinetics.

Interaction of cobicistat exposure on elvitegravir clearance

Interaction models were built up from the elvitegravir intermediate covariate model developed in the covariate analysis described above. First, *non-competitive* models integrating cobicistat (COBI) area under the concentration–time curve from 0 to 24 h (AUC_{COBI}) on apparent elvitegravir (EVG) clearance (CL/F_{EVG}) were assessed using linear, power and exponential functions, as follows:

$$\frac{CL}{F_{EVG}} = \frac{CL_0}{F_{EVG}} \times \left(1 - \theta_{COBI} \times \frac{AUC_{COBI} - \text{median } AUC_{COBI}}{\text{median } AUC_{COBI}}\right) \quad (1)$$

$$\frac{CL}{F_{EVG}} = \frac{CL_0}{F_{EVG}} \times \left(\frac{AUC_{COBI}}{\text{median } AUC_{COBI}}\right)^{-\theta_{COBI}} \quad (2)$$

$$\frac{CL}{F_{EVG}} = \frac{CL_0}{F_{EVG}} \times EXP\left(-\theta_{COBI} \times \frac{AUC_{COBI} - \text{median } AUC_{COBI}}{\text{median } AUC_{COBI}}\right) \quad (3)$$

where CL_0/F_{EVG} is the mean population CL/F_{EVG}, θ_{COBI} is the factor associated with the effect of cobicistat on CL/F_{EVG}. AUC_{COBI} was estimated at 9.8 mg·h/L in the study population using dose/CL/F_{COBI}, where CL/F_{COBI} is the apparent clearance of cobicistat in the final model.

Competitive models were then tested using linear, exponential and maximum-effect functions, as follows:

$$\frac{CL}{F_{EVG}} = \frac{CL_0}{F_{EVG}} \times I(t) \quad (4)$$

$$I(t) = 1 - (\theta_{COBI} \times C_{COBI}) \quad (5)$$

$$I(t) = EXP(-\theta_{COBI} \times C_{COBI}) \quad (6)$$

$$I(t) = 1 - \frac{C_{COBI} \times \theta_{Imax}}{\theta_{IC50} + C_{COBI}} \quad (7)$$

where $I(t)$ describes an inhibitory time-dependent model driven by cobicistat concentrations (C_{COBI}), θ_{COBI} is the factor associated with the effect of C_{COBI} on CL/F_{EVG}, θ_{Imax} is the maximum inhibitory effect of cobicistat and θ_{IC50} is the C_{COBI} producing 50% of the I_{max}.

Parameter estimation and model selection

All models were fitted using the first-order conditional estimation method with interaction (FOCEI). The log-likelihood ratio test, based on the reduction of the objective function value (ΔOFV) provided by NONMEM®, was used to discriminate between nested models. A decrease in OFV >3.84 ($P<0.05$) for one additional parameter in the structural model building was considered statistically significant (ΔOFV between any two nested models approximates a χ^2 distribution). To account for multiple testing in the covariate model (Bonferroni correction), a change in OFV >7.88 ($P<0.005$) was considered statistically significant for one additional parameter during model building and backward deletion steps, respectively. Goodness-of-fit plots, pharmacokinetic parameter precision and decrease in between-subject variability were further criteria considered for model selection. Reductions in the Akaike information criterion (ΔAIC) and the Bayesian information criterion value (ΔBIC) were also used to compare non-nested interaction models. Since a statistical interpretation cannot be given to ΔAIC or ΔBIC comparisons, we considered a decrease in AIC or BIC of 10 as strong evidence for considering one model over another.[29]

Model evaluation and assessment

The precision of the parameters was evaluated using non-parametric bootstrapping (1000 replicates) to generate 95% CIs for parameter estimates. A prediction-corrected visual predictive check (pcVPC) was also carried out using the PsN toolkit and Xpose (version 4.5.3).[30,31] Observed concentrations of elvitegravir and cobicistat were visually compared with the 5th, 50th and 95th percentiles of the simulated results. Figures were generated with R (Version 3.2.2, R Development Core Team, Foundation for Statistical Computing, Vienna, Austria, http://www.r-project.org/). An external validation was also performed using 48 samples collected from a separate group of 43 HIV-infected individuals treated with co-formulated elvitegravir between February and August 2015. Quantitative and categorical variables between the model-building and validation population groups were compared by means of the Mann–Whitney test and Fisher's exact test, respectively. Population and individual concentrations of elvitegravir and cobicistat were predicted based on the final models using the NONMEM® MAXEVAL=0 option. The predictive performance of the model was assessed in terms of bias (mean prediction error, MPE) and precision (root mean square prediction error, RMSE) and the associated 95% CI, as follows[32]:

$$MPE = \frac{\sum C_{pred} - C_{obs}}{N} \quad (8)$$

$$RMSE = \sqrt{\frac{\sum (C_{pred} - C_{obs})^2}{N}} \quad (9)$$

where C_{pred} represents population and individual predictions, C_{obs} the observed concentrations of the validation group and N the number of observations.

Simulations of standard and alternative dosage regimens

Elvitegravir/cobicistat (150/150 mg and 85/150 mg) with and without influencing co-medications were simulated with NONMEM® for 1000 individuals based on the final model estimates, including between- and within-subject variability. The median AUC_{COBI} of the study population was used as a covariate on CL/F_{EVG}. The 2.5th, 50th and 97.5th percentiles were calculated for each dosage regimen and graphically compared. Predicted elvitegravir C_{min}, C_{max} and AUC_{0-24} were estimated and used to calculate changes between different dosage regimens.

Results

A total of 186 and 167 observations were obtained for elvitegravir and cobicistat analyses, respectively. Participant demographic and clinical characteristics of the model-building and validation groups are summarized in Table 1. Only the proportion of male individuals was significantly different between the two datasets ($P=0.001$). Darunavir and atazanavir were the most frequent antiretroviral co-medications in all groups. No individuals treated with atazanavir received it in combination with ritonavir, likely due to cobicistat boosting. However, 8.3% and 9.3% of individuals in the model-building and validation groups, respectively, were treated with ritonavir-boosted darunavir (darunavir/r), thus adding a second boosting agent to the antiretroviral regimen.

Structural and covariate models for elvitegravir

A one-compartment model with first-order absorption and elimination fitted the data correctly. Models with two compartments or alternative absorption processes, including zero-order absorption

Table 1. Demographic and clinic characteristics of the study populations

Characteristic	Elvitegravir model-building group ($n=144$)	P	Cobicistat model-building group ($n=133$)	P	Model validation group ($n=43$)[a]
Sex (male), *n* (%)	111 (77.1)	0.01	105 (78.9)	0.005	24 (50.0)
Age (years), median (range)	41.0 (16–73)	0.09	41.5 (16–73)	0.10	45 (22–66)
Body weight (kg), median (range)	72 (45.8–125)	0.27	72 (50–125)	0.31	76 (45–110)
Height (cm), median (range)	175 (155–196)	0.27	175 (155–196)	0.22	173 (150–190)
Body surface area (m^2),[b] median (range)	1.9 (1.5–2.6)	0.66	1.9 (1.5–2.6)	0.68	1.9 (1.4–2.3)
Race, *n* (%)					
Caucasian	58 (40.3)		55 (41.4)		
African-American	13 (9.0)		12 (9.0)		
Hispanic	4 (2.8)		2 (1.5)		
Asian	4 (2.8)		2 (1.5)		
unknown	65 (45.1)		62 (46.6)		43 (100)
rs8175347, *n* (%)					
*UGT1A1*1/*1*	24 (16.7)				
*UGT1A1*1/*28*	27 (18.7)				
*UGT1A1*28/*28*	5 (3.5)				
unknown	88 (61.1)				43 (100)
Co-medications, *n* (%)					
darunavir	15 (10.4)	0.37	15 (11.3)	0.25	2 (4.7)
darunavir/ritonavir	12 (8.3)	0.76	11 (8.3)	0.76	4 (9.3)
atazanavir	7 (4.9)	0.15	6 (4.5)	0.14	5 (11.6)
zidovudine	1 (0.8)		1 (0.8)		
etravirine	4 (2.8)		3 (2.3)		
efavirenz	6 (4.2)		5 (3.8)		
nevirapine	1 (0.7)		1 (0.8)		
maraviroc	3 (2.1)		3 (2.3)		

P, comparison between variables in the model-building and validation population groups.
[a]In the model validation group the same number ($n=48$) of elvitegravir and cobicistat plasma concentrations were obtained.
[b]Calculated with the Mosteller formula.

and lag time or the combination of first and zero-order absorption models with and without lag time, did not improve the fit (ΔOFV >0.0). Between-subject variability was assigned to CL/F_{EVG}, with no further improvement upon its assignment to the elvitegravir apparent volume of distribution (V/F_{EVG}) (ΔOFV $=-0.3$) or the first-order elvitegravir absorption rate constant (k_{a_EVG}) (ΔOFV $=-0.6$). A combined proportional and additive model adequately described the residual error.

In univariate analyses, no demographic or clinical covariates tested showed any significant influence on CL/F_{EVG} (ΔOFV >-3.2). The analysis of the subset of patients with complete covariate information confirmed these findings (ΔOFV >-4.1). Concomitant administration of atazanavir significantly decreased CL/F_{EVG} by 54% (95% CI −7.5% to −30.5%) and reduced CL/F_{EVG} variability by 12.1% (ΔOFV $=-25.7$, $P<0.001$). Co-administration of darunavir/r was associated with a decrease of CL/F_{EVG} by 29.2% but this association did not reach statistical significance (95% CI −23.1% to 81.5%, ΔOFV $=-2.2$). Individuals in the *UGT1A1*28/*28* genetic group showed a 20% decrease in CL/F_{EVG} but the association was not statistically significant (95% CI −72.4% to 113%, ΔOFV $=-0.9$). Structural and intermediate pharmacokinetic model results for elvitegravir are summarized in Table 2.

Structural and covariate models for cobicistat

A one-compartment model with first-order absorption and elimination fitted the data well, whereas a two-compartment model and alternative absorption models including zero-order absorption and lag time did not improve the fit or were not retained due to the implausibility of the estimates (ΔOFV >-4.5). Between-subject variability was assigned to CL/F_{COBI}, with no further improvement when assigned to the cobicistat apparent volume of distribution (V/F_{COBI}) (ΔOFV $=13.8$). Despite the observed significant fit improvement (ΔOFV $=-13$), the variability in the first-order absorption rate constant for cobicistat (k_{a_COBI}) was not retained due to the poor precision of the estimate. Six observations of cobicistat were below the LLOQ (5 ng/mL), with corresponding elvitegravir concentrations measured within the expected range of concentrations. Consequently, we could not exclude these measurements for possible non-adherence. A combined proportional and additive model was selected to describe the residual error.

In univariate analyses, no demographic or clinical covariates tested showed any significant influence on CL/F_{COBI} (ΔOFV >-1.2). The analysis of the subset of patients with complete covariate information provided very similar results (ΔOFV >-0.1). Concomitant

Table 2. Parameter estimates of elvitegravir and cobicistat structural and intermediate pharmacokinetic models

	Structural population pharmacokinetic parameters		Intermediate covariate population pharmacokinetic parameters	
	estimate	RSE (%)	estimate	RSE (%)
Elvitegravir				
CL/F_{EVG} (L/h)	7.3	5.2	7.7	5.0
V/F_{EVG} (L)	49.0	44.3	68.2	17.3
k_{a_EVG} (h^{-1})	0.13	33.7	0.20	20.0
θ_{ATV_EVG}			−0.54	22.2
BSV CL/F_{EVG} (%)	38.8	15.2	34.1	12.9
additive residual error (ng/mL)	184	20.2	93.3	34.2
proportional residual error (%)	34.5	14.7	45.1	13.0
Cobicistat				
CL/F_{COBI} (L/h)	15.6	12.7	16.0	11.3
V/F_{COBI} (L)	91.9	18.8	88.3	15.2
k_{a_COBI} (h^{-1})	0.82	48.9	0.76	40.6
θ_{ATV_COBI}			−0.47	38.4
θ_{DRVr}			−0.27	30.1
BSV CL/F_{COBI} (%)	40.7	11.1	41.9	12.1
additive residual error (ng/mL)	2.5[a]		2.5[a]	
proportional residual error (%)	79.8	9.4	69.6	12.0

CL/F_{EVG}, elvitegravir apparent clearance; V/F_{EVG}, elvitegravir apparent volume of distribution; k_{a_EVG}, first-order elvitegravir absorption rate constant; θ_{ATV_EVG}, relative influence of atazanavir co-administration on CL/F_{EVG}; CL/F_{COBI}, cobicistat apparent clearance; V/F_{COBI}, cobicistat apparent volume of distribution; k_{a_COBI}, first-order cobicistat absorption rate constant; θ_{ATV_COBI}, relative influence of atazanavir co-administration on CL/F_{COBI}; θ_{DRVr}, relative influence of darunavir co-administration on CL/F_{COBI}; BSV, between-subject variability; RSE, relative standard error defined as SE/estimate, with the SE directly retrieved from NONMEM®.
[a]Additive part of cobicistat error model was fixed at $\sqrt{0.25 \times (\text{LLOQ})^2} = 2.5$ ng/mL to account for BLQ data.

administration of atazanavir and darunavir/r significantly reduced CL/F_{COBI} by 47.3% (95% CI −83.0% to −11.6%, ΔOFV = −8.0, $P < 0.005$) and 27.4% (95% CI −43.3% to −11.5%, ΔOFV = −8.3, $P < 0.005$), respectively. In multivariate analyses, both atazanavir and darunavir/r co-administration remained as significant covariates. Cobicistat pharmacokinetic model results are summarized in Table 2.

Elvitegravir and cobicistat interaction model

Models exploring the interaction of cobicistat exposure on CL/F_{EVG} are summarized in Table 3. A non-competitive influence of AUC_{COBI} on CL/F_{EVG} was better explained by a power function (Figure 1), which markedly improved the description of the data (ΔOFV = −65.5, $P < 0.001$ compared with the elvitegravir intermediate covariate model). A 2-fold increase in AUC_{COBI} induced a 46% reduction in CL/F_{EVG} and AUC_{COBI} decreased CL/F_{EVG} between-subject variability by 51.3%. Atazanavir coadministration was retained as a covariate after the backward deletion step (ΔOFV = 8.3, $P < 0.005$).

In the competitive models, the influence of cobicistat concentration on elvitegravir clearance was best described by a linear function and improved the fit as well (ΔOFV = −35.6, $P < 0.001$ compared with elvitegravir intermediate covariate model). Although there were no notable differences in goodness-of-fit plots and pharmacokinetic parameter precision between both non-competitive and competitive models, the former was chosen based on the AIC and BIC criterion (ΔAIC = ΔBIC = −29.9).[29] The final population pharmacokinetic parameters for elvitegravir and cobicistat are summarized in Table 4. Diagnostic plots for elvitegravir and cobicistat final models are shown in Figures S1 and S2 (available as Supplementary data at *JAC* Online).

Model validation

Of 1000 replicates analysed during the bootstrap analysis, 8.9% failed to minimize successfully and were excluded. Since all bootstrap median values were contained within the 95% CI, differing by <10% from the population estimates, the model was considered reliable. The pcVPC indicates that the final models described the data adequately, with <10% of points outside the 90% prediction interval (Figure 2). The external validation analysis showed a non-significant bias of 5% (95% CI −7% to 19%) with a precision of 54%, within the range of residual variability for elvitegravir individual predictions and of 6% (95% CI −8% to 22%) with a precision of 66% for population predictions. For cobicistat, a bias of −17% (95% CI −6.9% to −26%) was observed, indicating underpredicted individual concentrations, particularly evident during the absorption phase, with a precision of 56%, within the range of residual variability. A sub-analysis of predicted concentrations in the post-absorption phase, i.e. 10 h after dose administration, abolished the bias (−11%, 95% CI 0.4% to −21%). At the population level, a non-significant bias of −24% (95% CI 3% to −44%) was observed. These results indicate that the predictive performance of the model is adequate for the disposition phase but that the model slightly under-predicts peak concentrations.

Simulations of dosage regimens

The average predicted elvitegravir C_{min} after a standard 150 mg daily dosage regimen at steady state was 341 ng/mL (95% prediction interval 192.5–541.6 ng/mL). Predicted elvitegravir AUC_{0-24}, C_{max} and C_{min} increased by 10.5 mg·h/L (IQR 9.4–11.6 mg·h/L, average relative increase of 53.9%), 420 ng/mL (IQR 380.6–461.2 ng/mL, average relative increase of 35.5%) and 369 ng/mL (IQR 317.3–423.2 ng/mL, average relative increase of 112.5%), respectively, under 150/150 mg of elvitegravir/cobicistat co-administered with atazanavir compared with the regimen without atazanavir. The predicted concentration–time course of 85/150 mg of elvitegravir/cobicistat co-administered with atazanavir overlapped the 150/150 mg of elvitegravir/cobicistat concentration–time profile (Figure 3). Predicted elvitegravir AUC_{0-24} and C_{max} decreased by 2.5 mg·h/L (IQR 2.2–2.8 mg·h/L, average relative decrease of 12.82%) and 274 ng/mL (IQR 260.2–287.8 ng/mL, average relative decrease of 23.2%), respectively, while predicted elvitegravir C_{min} increased by 66.2 ng/mL (IQR 63.6–67.3 ng/mL, average relative increase of 20.4%) under

Table 3. Non-competitive and competitive models used to explore the influence of cobicistat exposure on elvitegravir apparent clearance

Function	Model: $CL/F_{EVG} \times I$[a]	CL/F_{EVG} (RSE)	θ_{COBI} (RSE)	ΔOFV[b]	*P*	ΔAIC[b]	ΔBIC[b]
Linear	$I = \left(1 - \theta_{COBI} \times \frac{AUC_{COBI} - \text{median } AUC_{COBI}}{\text{median } AUC_{COBI}}\right)$	7.7 (4.7)	0.50 (10.3)	−45.1	<0.001	−43.1	−39.2
Power[c]	$I = \left(\frac{AUC_{COBI}}{\text{median } AUC_{COBI}}\right)^{-\theta_{COBI}}$	7.6 (4.4)	1.12 (14.9)	−65.5	<0.001	−63.5	−59.6
Exponential	$I = \left(-\theta_{COBI} \times \frac{AUC_{COBI} - \text{median } AUC_{COBI}}{\text{median } AUC_{COBI}}\right)$	7.7 (4.6)	0.92 (17.3)	−63.1	<0.001	−61.1	−57.2
Linear	$I = 1 - \theta_{COBI} \times C_{COBI}$	13.6 (18.8)	1.18 (26.4)	−35.6	<0.001	−33.6	−29.7
Exponential	$I = EXP(-\theta_{COBI} \times C_{COBI})$	13 (14.1)	1.88 (34.7)	−32.8	<0.001	−30.8	−27.0
Maximum effect	$I = 1 - \frac{C_{COBI} \times \theta_{Imax}}{\theta_{IC50} + C_{COBI}}$	12.6 (13.6)	0.381[d] (40.7)	−30.4	<0.001	−28.4	−24.6

ΔOFV, difference in the NONMEM® objective function value; ΔAIC, difference in the Akaike information criterion; ΔBIC, difference in the Bayesian information criterion or Schwarz criterion; CL/F_{EVG}, elvitegravir apparent clearance (L/h); AUC_{COBI}, cobicistat area under the concentration–time curve from 0 to 24 h; C_{COBI}, cobicistat plasma concentration at each timepoint; θ_{COBI}, factor associated with the effect of cobicistat pharmacokinetics on CL/F_{EVG}; θ_{Imax}, maximum inhibitory effect of cobicistat fixed to 1 as no consistent estimate could be obtained; θ_{IC50}, estimate of cobicistat concentration (ng/mL) producing 50% of the I_{max}; RSE, relative standard error expressed as percentage and defined as SE/estimate, with SE directly retrieved from NONMEM®.

[a]*I* describes an inhibitory model induced by cobicistat exposures or timepoint concentrations.

[b]Compared with elvitegravir intermediate covariate model.

[c]Non-competitive model included in elvitegravir final population pharmacokinetic model.

[d]θ_{IC50}.

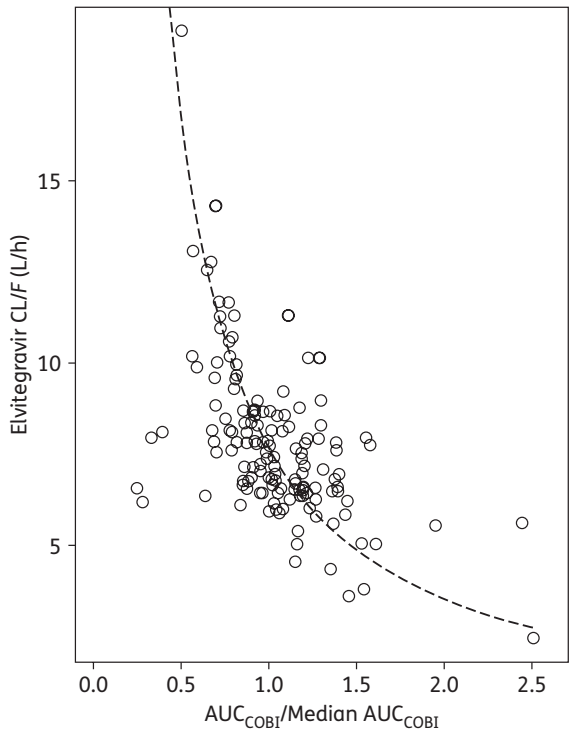

Figure 1. Elvitegravir elimination as a function of cobicistat exposure. Open circles represent individual elvitegravir apparent clearance (CL/F_{EVG}) plotted versus cobicistat exposure (AUC_{COBI}) centred on the median value, obtained from the cobicistat final pharmacokinetic model. The broken line corresponds to the population median prediction from the final power function model.

85/150 mg of elvitegravir/cobicistat compared with the standard regimen without atazanavir.

Discussion

Our study provides a description of the population pharmacokinetic profile of elvitegravir and cobicistat in a real patient setting, allowing simulations of standard and alternative dosage regimens. These population pharmacokinetic models can be used to derive percentile reference curves or implemented in a Bayesian tool for dosage adjustment. The CL/F_{EVG} pharmacokinetic estimate is close to reported values of 6.6–7.1 L/h, while V/F_{EVG} is much lower than previously published values of 137.9–197.9 L, probably due to study design distinctions, since data were collected over a 28 h period, hindering the estimation of an extensive drug distribution in peripheral tissues.[18] Although the elvitegravir absorption phase could not be exhaustively described, with scarce measurements available within a few hours after drug administration, a mean absorption time of about 6 h is comparable to values obtained with other more complex published models.[18] The CL/F_{COBI} and V/F_{COBI} pharmacokinetic estimates are in good agreement with previously reported values of 15.0 L/h and 77.0 L, respectively.[19] Similarly, the cobicistat mean absorption time of 1.9 h is close to values obtained with more comprehensive absorption models.[19] None of the demographic and clinical covariates tested appeared to have a significant impact on elvitegravir and cobicistat elimination, in contrast to results suggesting statistically significant, although not clinically relevant, influences of body surface area on CL/F_{EVG} and of body weight on CL/F_{COBI}.[18,19] This could be explained by the lack of extreme body surface area values in our study population.

Table 4. Final population pharmacokinetic parameters for elvitegravir and cobicistat with bootstrap results

	Final population pharmacokinetic parameters		Bootstrap (n=1000 samples)	
	estimate	RSE (%)	median	95% CI
Elvitegravir				
CL/F_{EVG} (L/h)	7.6	4.4	7.6	6.9–8.3
V/F_{EVG} (L)	61.0	16.7	62.8	36.1–111.5
k_{a_EVG} (h^{-1})	0.17	16.4	0.17	0.11–0.52
θ_{ATV_EVG}	−0.35	25.7	−0.36	−0.55 to −0.14
θ_{AUC_COBI}	1.12	14.9	1.13	1.50–0.66
BSV CL/F_{EVG} (%)	16.6	31.2	18.3	4.8–30.6
additive residual error (ng/mL)	148	28.0	133	15.1–231
proportional residual error (%)	39.8	10.9	38.4	26.9–47.3
Cobicistat				
CL/F_{COBI} (L/h)	16.0	11.3	15.9	12.7–20.0
V/F_{COBI} (L)	88.3	15.2	84.3	49.0–116.7
k_{a_COBI} (h^{-1})	0.76	40.6	0.75	0.24–1.24
θ_{ATV_COBI}	−0.47	38.4	−0.47	−0.70 to −0.19
θ_{DRVr}	−0.27	30.1	−0.27	−0.42 to −0.09
BSV CL/F_{COBI} (%)	41.9	12.1	41.5	24.7–53.6
additive residual error (ng/mL)	2.5[a]		2.5[a]	
proportional residual error (%)	69.6	12.0	68.3	54.0–86.1

Final elvitegravir model: $CL/F_{EVG}\ (L/h) = 7.6 \times (1 - 0.35 \times ATV) \times (AUC_{COBI}/\text{median}\,AUC_{COBI})^{-1.12}$.
Final cobicistat model: $CL/F_{COBI}(L/h) = 16.0 \times (1 - 0.47 \times ATV) \times (1 - 0.27 \times DRVr)$.
CL/F_{EVG}, elvitegravir apparent clearance; V/F_{EVG}, elvitegravir apparent volume of distribution; k_{a_EVG}, first-order elvitegravir absorption rate constant; θ_{ATV_EVG}, relative influence of atazanavir co-administration on CL/F_{EVG}; θ_{AUC_COBI}, relative influence of cobicistat AUC (AUC_{COBI}) on CL/F_{EVG} following a power function; CL/F_{COBI}, cobicistat apparent clearance; V/F_{COBI}, cobicistat apparent volume of distribution; k_{a_COBI}, first-order cobicistat absorption rate constant; θ_{ATV_COBI}, relative influence of atazanavir co-administration on CL/F_{COBI}; θ_{DRVr}, relative influence of darunavir/r co-administration on CL/F_{COBI}; BSV, estimate of between-subject variability; RSE, relative standard error defined as SE/estimate, with standard error (SE) directly retrieved from NONMEM®.
[a]Additive part of cobicistat error model was fixed to $\sqrt{0.25 \times (LLOQ)^2} = 2.5$ ng/mL to account for BLQ data.

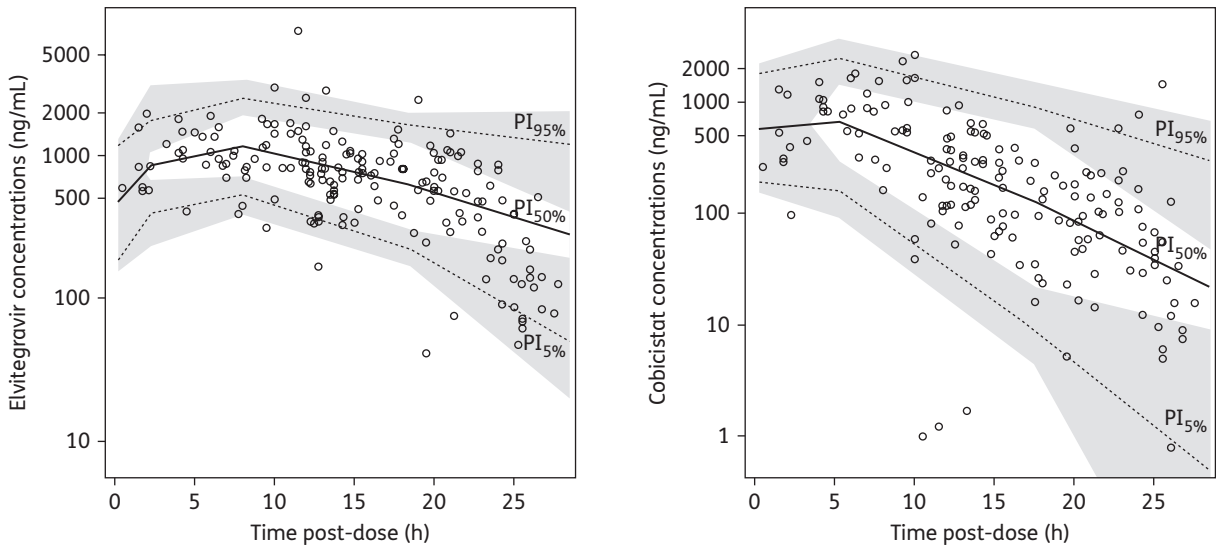

Figure 2. pcVPC of the elvitegravir (n=186) and cobicistat (n=167) final model. Open circles represent elvitegravir (left-hand panel) and cobicistat (right-hand panel) plasma concentrations. The continuous line represents the population median prediction from the final model and the broken lines represent the 90% prediction intervals. PI, prediction interval.

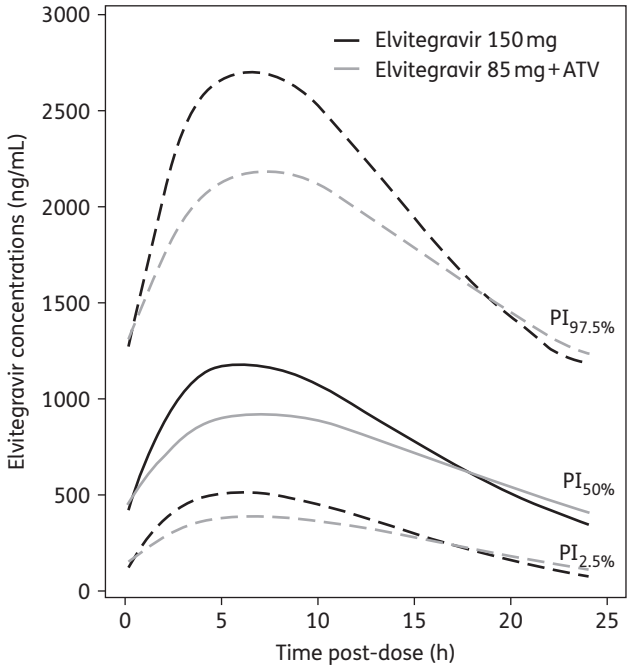

Figure 3. Elvitegravir simulated plasma concentrations for dosage regimens of 150 and 85 mg using median cobicistat AUC (AUC_{COBI}) and atazanavir co-administration as covariates on elvitegravir clearance. Continuous lines represent the population median prediction for 150 mg (black) and 85 mg (grey) regimens. Dashed lines represent the 95% prediction intervals for the 150 mg (black) and 85 mg (grey) regimens. ATV, atazanavir; PI, prediction interval.

The results of our study highlight relevant drug interactions likely to be encountered in routine clinical practice. The significant impact of concomitant atazanavir on CL/F_{EVG} is likely explained by the known atazanavir-mediated inhibition of UGT1A1, an enzyme that mediates the secondary metabolic pathway of elvitegravir.[33] The interaction between ritonavir-boosted elvitegravir and atazanavir was evaluated in the early stages of elvitegravir development, showing significantly higher elvitegravir exposures when 200/100 mg of elvitegravir/ritonavir was co-administered with 300 mg of atazanavir.[10] Hence, a reduced dose of 85 mg of elvitegravir was finally selected for the combination with 300/100 mg of atazanavir/ritonavir and recently commercialized in some countries.[9] Our results confirm the interaction between elvitegravir and atazanavir and validate the dose adjustment proposed for the combination of elvitegravir with atazanavir boosted with ritonavir or cobicistat. As shown in previous interaction studies, our simulations predicted a slightly higher C_{min} but lower C_{max} and AUC_{0-24} for the adapted elvitegravir dosage regimen, probably of limited clinical relevance.[10] The question remains whether the same elvitegravir dose adjustment is suitable with co-administration of 400 mg of atazanavir, since only one individual in the study population was under this dosage regimen.

Homozygosity for the allele *UGT1A1*28* led to a mild reduction in CL/F_{EVG}, which was statistically non-significant, probably due to the small sample size.[34] A 20% reduction in CL/F_{EVG} might not be clinically relevant compared with the moderate between-subject variability, but should be confirmed in larger studies.[34]

Atazanavir and darunavir are known to inhibit CYP3A4, which mediates the main metabolic pathway of cobicistat and explains the influence of both drugs on CL/F_{COBI}.[33,35] These drug–drug interactions might also have an indirect impact on elvitegravir pharmacokinetics. The effect of atazanavir on CL/F_{EVG} is probably explained both indirectly by the increase in cobicistat exposure and by the direct UGTA1A inhibition. None of these covariates decreased between-subject variability of CL/F_{COBI}, probably due to difficulties in distinguishing between- from within-subject variability in our analysis, which included only one observation for most individuals.

Published data on cobicistat-boosted elvitegravir did not show a significant effect of AUC_{COBI} on elvitegravir clearance. However, ritonavir AUC_{0-24} (dose ranging from 100 to 200 mg) had a statistically significant but clinically irrelevant effect on elvitegravir bioavailability.[18] In our study, AUC_{COBI} showed a marked influence on elvitegravir elimination when modelled as a non-competitive inhibitor. Notably, this effect explained up to half of the elvitegravir between-subject variability. A reduction of AUC_{COBI} by 25%, 50% and 75% would drive an increase in CL/F_{EVG}, and therefore a reduction in elvitegravir exposure of 38.0%, 117.3% and 372.4%, respectively. These results emphasize the need for a careful examination of co-medications modulating CYP3A4 activity that could directly and indirectly affect elvitegravir concentrations.

Elvitegravir antiviral effect was supported by a Phase 2 study in which ritonavir-boosted elvitegravir C_{min} values exceeded the protein-binding-adjusted 95% inhibitory concentration (IC_{95}) of 45 ng/mL and were associated with viral suppression over 10 days (2 log reduction from baseline in HIV-1 RNA copies).[36] No association between elvitegravir exposure and virological response by week 48 was found in Phase 3 pharmacokinetic–pharmacodynamic studies and no therapeutic target, apart from the IC_{95}, has been defined to date.[37] Model-based simulated minimal concentrations suggest that all individuals will present concentrations above the IC_{95} and would be at low risk of virological failure with the recommended dosage regimen. On the other hand, one might conjecture whether a proportion of individuals might be exposed to concentrations higher than the required levels without any substantial benefit, but possibly with undesirable consequences in the long term. However, there is currently no clinical evidence to support a cumulative toxicity of elvitegravir.

In conclusion, the variability in elvitegravir pharmacokinetics is modest after accounting for variations in cobicistat exposure. Drug–drug interactions that might be encountered in daily practice might lead to inadequate elvitegravir levels and monitoring of plasma concentrations could be a useful tool to identify patients at risk of suboptimal concentrations.

Acknowledgements

We thank the individuals who participate in the SHCS, the physicians and study nurses for excellent patient care and the technicians of the Laboratory of Clinical Pharmacology, Service of Biomedicine, University Hospital Centre of Lausanne.

Members of the Swiss HIV Cohort Study

Aubert V, Battegay M, Bernasconi E, Böni J, Braun DL, Bucher HC, Burton-Jeangros C, Calmy A, Cavassini M, Dollenmaier G, Egger M, Elzi L, Fehr J, Fellay J, Furrer H (Chairman of the Clinical and Laboratory Committee),

Fux CA, Gorgievski M, Günthard H (President of the SHCS), Haerry D (deputy of 'Positive Council'), Hasse B, Hirsch HH, Hoffmann M, Hösli I, Kahlert C, Kaiser L, Keiser O, Klimkait T, Kouyos R, Kovari H, Ledergerber B, Martinetti G, Martinez de Tejada B, Marzolini C, Metzner K, Müller N, Nadal D, Nicca D, Pantaleo G, Rauch A (Chairman of the Scientific Board), Regenass S, Rudin C (Chairman of the Mother & Child Substudy), Schöni-Affolter F (Head of Data Centre), Schmid P, Speck R, Stöckle M, Tarr P, Trkola A, Vernazza P, Weber R, Yerly S.

Funding

This work was supported by Fundación Alfonso Martínez Escudero (private foundation scholarship MAD-1-2-105 to C. B.), the Swiss National Science Foundation (research project FNRS 324730_141234 to L. A. D. and research project from Nano-Tera Program 20NA21—145955 to T. B., L. A. D. and C. C.) and the Swiss HIV Cohort Study (research project SHCS 764 to M. C.). The data are gathered by the five Swiss University Hospitals, two Cantonal Hospitals, 15 affiliated hospitals and 36 private physicians (listed at http://www.shcs.ch/180-health-care-providers). Part of the data was generated during the routine work of the University Hospital of Lausanne.

Transparency declarations

None to declare.

Supplementary data

Figures S1 and S2 are available as Supplementary data at *JAC* Online (http://jac.oxfordjournals.org/).

References

1 *Stribild (Package Insert)*. http://www.gilead.com/~/media/files/pdfs/medicines/hiv/stribild/stribild_pi.pdf?la=en.

2 DeJesus E, Rockstroh JK, Henry K *et al*. Co-formulated elvitegravir, cobicistat, emtricitabine, and tenofovir disoproxil fumarate versus ritonavir-boosted atazanavir plus co-formulated emtricitabine and tenofovir disoproxil fumarate for initial treatment of HIV-1 infection: a randomised, double-blind, phase 3, non-inferiority trial. *Lancet* 2012; **379**: 2429–38.

3 Sax PE, DeJesus E, Mills A *et al*. Co-formulated elvitegravir, cobicistat, emtricitabine, and tenofovir versus co-formulated efavirenz, emtricitabine, and tenofovir for initial treatment of HIV-1 infection: a randomised, double-blind, phase 3 trial, analysis of results after 48 weeks. *Lancet* 2012; **379**: 2439–48.

4 Molina JM, Lamarca A, Andrade-Villanueva J *et al*. Efficacy and safety of once daily elvitegravir versus twice daily raltegravir in treatment-experienced patients with HIV-1 receiving a ritonavir-boosted protease inhibitor: randomised, double-blind, phase 3, non-inferiority study. *Lancet Infect Dis* 2012; **12**: 27–35.

5 Pozniak A, Markowitz M, Mills A *et al*. Switching to coformulated elvitegravir, cobicistat, emtricitabine, and tenofovir versus continuation of non-nucleoside reverse transcriptase inhibitor with emtricitabine and tenofovir in virologically suppressed adults with HIV (STRATEGY-NNRTI): 48 week results of a randomised, open-label, phase 3b non-inferiority trial. *Lancet Infect Dis* 2014; **14**: 590–9.

6 Arribas JR, Pialoux G, Gathe J *et al*. Simplification to coformulated elvitegravir, cobicistat, emtricitabine, and tenofovir versus continuation of ritonavir-boosted protease inhibitor with emtricitabine and tenofovir in adults with virologically suppressed HIV (STRATEGY-PI): 48 week results of a randomised, open-label, phase 3b, non-inferiority trial. *Lancet Infect Dis* 2014; **14**: 581–9.

7 Panel on Antiretroviral Guidelines for Adults and Adolescents. *Guidelines for the Use of Antiretroviral Agents in HIV-1-Infected Adults and Adolescents*. US Department of Health and Human Services, 2015.

8 Panel on Antiretroviral Guidelines for Adults and Adolescents. *European Guidelines for Treatment of HIV-Infected Adults in Europe*. European AIDS Clinical Society (EACS), 2014.

9 *Vitekta (Package Insert)*. http://www.accessdata.fda.gov/drugsatfda_docs/label/2014/203093s000lbl.pdf.

10 Ramanathan S, Mathias AA, German P *et al*. Clinical pharmacokinetic and pharmacodynamic profile of the HIV integrase inhibitor elvitegravir. *Clin Pharmacokinet* 2011; **50**: 229–44.

11 FDA. *Stribild® (Elvitegravir/Cobicistat/Tenofovir Disoproxil Fumarate/Emtricitabine) Tablets: Clinical Pharmacology and Biopharmaceutical Review*. http://www.accessdata.fda.gov/drugsatfda_docs/nda/2012/203100Orig1s000ClinPharmR.pdf.

12 Raffe S, Fisher M. The pharmacokinetics, pharmacodynamics and clinical efficacy of elvitegravir + cobicistat + emtricitabine + tenofovir combination therapy for the treatment of HIV. *Expert Opin Drug Metab Toxicol* 2015; **11**: 427–35.

13 *Evotaz (Package Insert)*. http://packageinserts.bms.com/pi/pi_evotaz.pdf.

14 *Prezcobix (Package Insert)*. http://www.accessdata.fda.gov/drugsatfda_docs/label/2015/205395s000lbl.pdf.

15 *Tybost (Package Insert)*. http://www.gilead.com/~/media/files/pdfs/medicines/hiv/tybost/tybost_pi.pdf?la=en.

16 Deeks ED. Cobicistat: a review of its use as a pharmacokinetic enhancer of atazanavir and darunavir in patients with HIV-1 infection. *Drugs* 2014; **74**: 195–206.

17 Shah BM, Schafer JJ, Priano J *et al*. Cobicistat: a new boost for the treatment of human immunodeficiency virus infection. *Pharmacotherapy* 2013; **33**: 1107–16.

18 Custodio JM, Gordi T, Zhong L *et al*. Population pharmacokinetics of boosted-elvitegravir in HIV-infected patients. *J Clin Pharmacol* 2015; doi:10.1002/jcph.657.

19 Custodio JM, Gordi T, Kearney BP *et al*. Population pharmacokinetics of cobicistat in adult healthy subjects and HIV-infected patients. In: *Abstracts of the Fourteenth International Workshop on Clinical Pharmacology of HIV Therapy, 2013*. Abstract P_36.

20 Aouri M, Calmy A, Hirschel B *et al*. A validated assay by liquid chromatography-tandem mass spectrometry for the simultaneous quantification of elvitegravir and rilpivirine in HIV positive patients. *J Mass Spectrom* 2013; **48**: 616–25.

21 Monaghan G, Ryan M, Seddon R *et al*. Genetic variation in bilirubin UPD-glucuronosyltransferase gene promoter and Gilbert's syndrome. *Lancet* 1996; **347**: 578–81.

22 Liu X, Xu W. UGT1A1*28 polymorphisms: a potential pharmacological biomarker of irinotecan-based chemotherapies in colorectal cancer. *Pharmacogenomics* 2014; **15**: 1171–4.

23 Rotger M, Taffe P, Bleiber G *et al*. Gilbert syndrome and the development of antiretroviral therapy-associated hyperbilirubinemia. *J Infect Dis* 2005; **192**: 1381–6.

24 Beutler E, Gelbart T, Demina A. Racial variability in the UDP-glucuronosyltransferase 1 (UGT1A1) promoter: a balanced polymorphism for regulation of bilirubin metabolism? *Proc Natl Acad Sci USA* 1998; **95**: 8170–4.

25 Beal SL. Ways to fit a PK model with some data below the quantification limit. *J Pharmacokinet Pharmacodyn* 2001; **28**: 481–504.

26 Ahn JE, Karlsson MO, Dunne A *et al*. Likelihood based approaches to handling data below the quantification limit using NONMEM VI. *J Pharmacokinet Pharmacodyn* 2008; **35**: 401–21.

27 Bergstrand M, Karlsson MO. Handling data below the limit of quantification in mixed effect models. *AAPS J* 2009; **11**: 371–80.

28 Xu XS, Dunne A, Kimko H *et al*. Impact of low percentage of data below the quantification limit on parameter estimates of pharmacokinetic models. *J Pharmacokinet Pharmacodyn* 2011; **38**: 423–32.

29 Kass RE, Raftery AE. Bayes factors. *J Am Stat Assoc* 1995; **90**: 773–95.

30 Jonsson EN, Karlsson MO. Xpose—an S-PLUS based population pharmacokinetic/pharmacodynamic model building aid for NONMEM. *Comput Methods Programs Biomed* 1999; **58**: 51–64.

31 Lindbom L, Pihlgren P, Jonsson EN. PsN-Toolkit—a collection of computer intensive statistical methods for non-linear mixed effect modeling using NONMEM. *Comput Methods Programs Biomed* 2005; **79**: 241–57.

32 Sheiner LB, Beal SL. Some suggestions for measuring predictive performance. *J Pharmacokinet Biopharm* 1981; **9**: 503–12.

33 *Reyataz (Package Insert)*. http://www.accessdata.fda.gov/drugsatfda_docs/label/2011/021567s025lbl.pdf.

34 Custodio JM, Guo S, Graham H *et al*. Pharmacokinetics and safety of cobicistat boosted-elvitegravir in subjects with decreased UGT1A1 activity. In: *Abstracts of the Fifteenth International Workshop on Clinical Pharmacology of HIV & Hepatitis Therapy, 201*4. Abstract P_40.

35 *Prezista (Package Insert)*. http://www.accessdata.fda.gov/drugsatfda_docs/label/2012/021976s021lbl.pdf.

36 DeJesus E, Berger D, Markowitz M *et al*. Antiviral activity, pharmacokinetics, and dose–response of the HIV-1 integrase inhibitor GS-9137 (JTK-303) in treatment-naive and treatment-experienced patients. *J Acquir Immune Defic Syndr* 2006; **43**: 1–5.

37 EMA. *EMA/332263/2013 Stribild Assessment Report*. http://www.ema.europa.eu/docs/en_GB/document_library/EPAR_-_Public_assessment_report/human/002574/WC500144274.pdf.